

Research Article

Dynamic Analysis of Wind Turbine Driven Self-excited Induction Generator

¹K. Premalatha and ²S. Vasantharathna

¹Department of EEE, Kumaraguru College of Technology, Coimbatore, Tamil Nadu 641049,

²Department of EEE, Coimbatore Institute of Technology, Coimbatore, Tamil Nadu 641014, India

Abstract: This study presents the dynamic performance of stand-alone self-excited induction generator driven by a variable speed wind turbine using direct torque control strategy. The system consists of wind turbine, self-excited induction generator, voltage source converter and battery with capacitor. The input to the induction generator is wind whose velocity is not constant. The magnitude and frequency of the generator terminal voltage varies with wind velocity. To maintain the voltage and frequency of the induction generator terminal constant; the direct torque control strategy is used. This study investigates the dynamic and steady state performance of self-excited induction generator for varying load and wind speed conditions and short circuit at stator terminals. The proposed system is designed and simulated in MATLAB/SIMULINK environment. The simulation results show the effectiveness of the proposed system.

Keywords: Direct torque control, self-excited induction generator, voltage source converter, wind energy conversion system

INTRODUCTION

It is common fact that the renewable energy resources are considered to be an alternative source for the conventional resources. Among the renewable energy resources, the most prized is wind energy source because of the following reasons; efficient, clean and safe, availability is plentiful, less running cost and maintenance etc. Nowadays, Wind Energy Conversion Systems (WECS) are employed for supplying power to the remote areas and villages (Daniel and Ammasaigounden, 2004; Infield *et al.*, 1983). There are several types of wind generators available to convert the wind energy into useful form. But, the choice is made on the induction generator because of its advantages like reliable, cheap, light weight, having simple construction and requires very little maintenance (Vas, 1998; Patil *et al.*, 2014).

The wind velocity fluctuates on hourly and daily basis. Therefore, the magnitude and frequency of the induction generator terminal voltage varies. To control the voltage and frequency of the Self Excited Induction Generator (SEIG), the standalone system needs an interface to convert the variable voltage variable frequency AC of the generator to the fixed voltage fixed frequency AC at the utility. To achieve this, two fully controlled converters are used and the converters are rated at least to the generator power. The problem with the arrangement is that, it requires complex control (Honorati *et al.*, 1996). The induction generator is

capable of self-excitation when, in order to supply reactive power either by using capacitor bank or by an inverter assisted battery. Capacitor banks are used to supply reactive power for SEIG only when there is an initial voltage on the capacitor bank or residual flux present in the machine core and also have poor voltage regulation and frequency variation under variable wind speed conditions (Grantham *et al.*, 1989; Leidhold *et al.*, 2002). A PWM-VSI scheme with a battery bank and a DC-charged capacitor is used for excitation and voltage control, but it gives slow response (Jayaramaiah and Fernandes, 2006). Ojo and Davidson (2000), Seyoum *et al.* (2003) and Mateo and Vukadinovic (2013) presented the stator field oriented control for the voltage control and excitation of SEIG using Voltage Source Converter (VSC) with battery. Korkmaz *et al.* (2013) and Aymen and Lassaad (2012) presented vector control methods for WECS. But, the vector control methods require co-ordinate transformations, current controllers and decoupling of stator flux and torque producing components. The system performance is affected by the induction generator parameter variations.

To overcome the above mentioned problems Direct Torque Control (DTC) strategy is proposed. DTC has a simple control scheme, good dynamic behaviour and the problem of decoupling the stator flux and torque components can be avoided. In DTC strategy, only the stator resistance is needed to estimate the stator flux and torque. DTC requires less computational

Corresponding Author: K. Premalatha, Department of Electrical and Electronics Engineering, Kumaraguru College of Technology, Coimbatore, Tamil Nadu 641049, India

This work is licensed under a Creative Commons Attribution 4.0 International License (URL: <http://creativecommons.org/licenses/by/4.0/>).

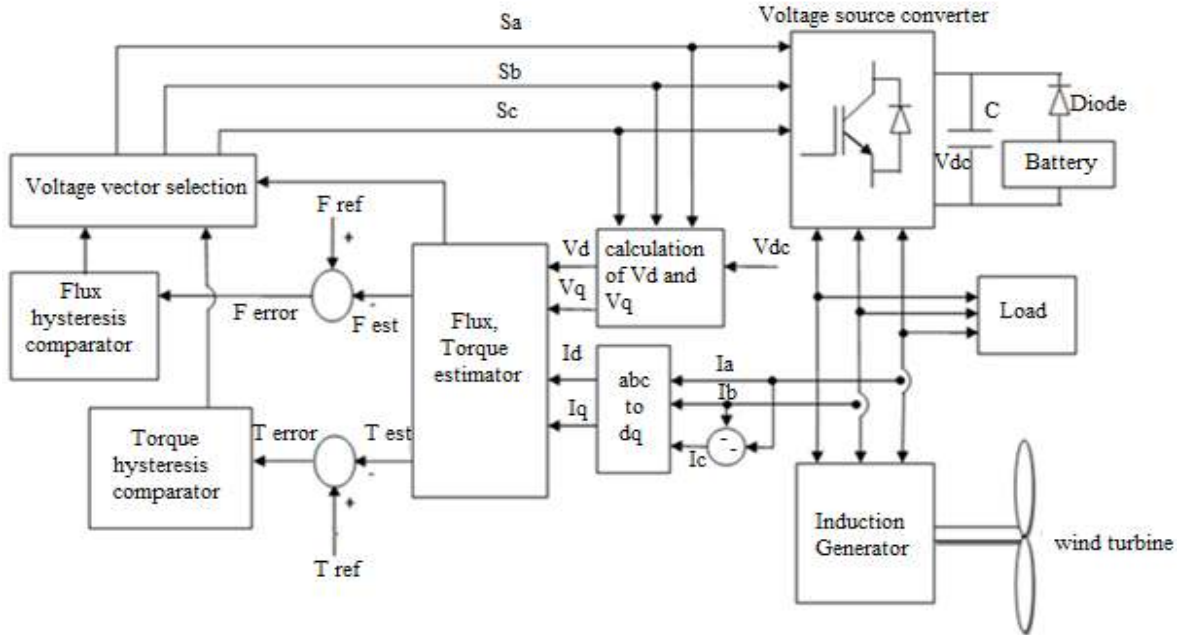


Fig. 1: System configuration

power (Patil *et al.*, 2014; Bose, 2003; Takahashi and Noguchi, 1986; Depenbrock, 1988). This study presents the dynamic and steady state analysis of SEIG used for variable speed WECS using DTC switching strategy.

SYSTEM CONFIGURATION

Figure 1 shows the block diagram of the proposed system. The system consists of SEIG, wind turbine with step up gear box, battery, VSC with a capacitor and loads. The battery is used to charge the capacitor. The excitation for SEIG is given through VSC and battery. SEIG terminals are directly joined to AC side of the VSC. DC side of the converter is connected to battery. The VSC output is of constant amplitude and frequency which forms a local grid for supplying SEIG. DTC strategy is used for generating gate pulses for the VSC.

The direct and quadrature axis voltages are obtained from the switching functions and DC link voltage. Using the DC voltage and measured stator currents, stator flux, electromagnetic torque and position of stator flux are estimated. Now the estimated torque and flux are compared with their respective reference values. The torque error is processed using torque hysteresis comparator. Similarly, flux error is processed using flux hysteresis comparator. The output of the torque and flux hysteresis comparators along with the stator flux position are given to the voltage vector selection table and from which the required voltage switching vector is selected. According to the voltage vector selected, the power switches of the VSC are switched on and off and the output voltage is maintained at a constant value irrespective of wind

velocity variations and load condition. When the generated power is more than the load demand, the excess power is used for charging the battery or it would be dissipated in the dump resistor.

Modelling of SEIG: The dynamic model of the induction machine in an arbitrary reference frame (Krause *et al.*, 2002) is given in Eq. (1)-(5):

$$R_s I_s + \frac{d\psi_s}{dt} = v_s \quad (1)$$

$$R_r I_r + \frac{d\psi_r}{dt} = 0 \quad (2)$$

$$\bar{\psi}_s = L_s \bar{I}_s + L_m \bar{I}_r \quad (3)$$

$$\bar{\psi}_r = L_r \bar{I}_r + L_m \bar{I}_s \quad (4)$$

$$T_e = \frac{3P}{2} \frac{L_m}{\sigma L_s L_r} \bar{\psi}_r * \bar{\psi}_s \quad (5)$$

where,

- R_s, R_r = The stator and rotor resistances
- L_s and L_r = The self-inductances of stator and rotor
- L_m = The mutual inductance
- P = The number of poles
- σ = Leakage factor

Modelling of voltage source converter: The three phase VSC converts AC to DC and vice versa. It consists of six insulated gate bipolar transistors with anti-parallel diodes. The output voltage of VSC can be obtained using switching functions and DC voltage (Lee and Ehsani, 2001). The AC side voltage of the VSC is given in (6):

$$\begin{bmatrix} V_a \\ V_b \\ V_c \end{bmatrix} = \frac{V_{DC}}{3} \begin{bmatrix} 2 & -1 & -1 \\ -1 & 2 & -1 \\ -1 & -1 & 2 \end{bmatrix} * \begin{bmatrix} S_A \\ S_B \\ S_C \end{bmatrix} \quad (6)$$

The voltage in d-q coordinate system is:

$$V_{sd} = \left(\frac{2}{3}S_A - \frac{1}{3}S_B - \frac{1}{3}S_C \right) * V_{DC} \quad (7)$$

$$V_{sq} = \left(-\frac{1}{\sqrt{3}}S_B + \frac{1}{\sqrt{3}}S_C \right) * V_{DC} \quad (8)$$

DIRECT TORQUE CONTROL SCHEME

The d-q axis stator flux is obtained by integrating the direct and quadrature axis voltages are obtained by subtracting the ohmic drop:

$$\bar{\Psi}_{ds}^s = \int (V_{ds}^s - I_{ds}^s R_s) dt \quad (9)$$

$$\bar{\Psi}_{qs}^s = \int (V_{qs}^s - I_{qs}^s R_s) dt \quad (10)$$

The stator flux $\bar{\Psi}_s$ is given by:

$$\bar{\Psi}_s = \sqrt{(\bar{\Psi}_{ds}^s)^2 + (\bar{\Psi}_{qs}^s)^2} \quad (11)$$

The stator flux angle is given by:

$$\theta_e(k) = \tan^{-1} \frac{\bar{\Psi}_{ds}^s}{\bar{\Psi}_{qs}^s} \quad (12)$$

The electromagnetic torque developed by the machine is estimated using d-q axis currents and fluxes:

$$T_e = \frac{3P}{22} (\Psi_{ds}^s I_{qs}^s - \Psi_{qs}^s I_{ds}^s) \quad (13)$$

Flux and torque hysteresis comparator: The reference flux (Ψ_s^*) is compared with calculated flux

(Ψ_s) and the flux error $\Delta\Psi_s$ is given to the flux hysteresis comparator. The flux error is:

$$\Delta\Psi_s = \Psi_s^* - \Psi_s \quad (14)$$

The flux hysteresis comparator has two levels of digital output 1 and -1 and the relation is given in Table 1.

The reference torque (T_e^*) is compared with the calculated torque (T_e) and the torque error ΔT_e is given to the torque hysteresis comparator. The torque error is:

$$\Delta T_e = T_e^* - T_e \quad (15)$$

The torque hysteresis comparator has three levels of digital output 1, 0 and -1 and the relation is given in Table 2.

When the reference torque is greater than the calculated torque, the output is 1 and torque has to be increased whereas if the calculated torque is greater than the reference torque, then output is -1 and torque has to be decreased. If zero, there is no change in torque.

Table 1: Switching logic for flux error

State	Flux hysteresis comparator output
$(\Psi_s^* - \Psi_s) > \Delta\Psi_s$	1 ↑
$(\Psi_s^* - \Psi_s) < -\Delta\Psi_s$	-1 ↓

Table 2: Switching logic for torque error

State	Torque hysteresis comparator output
$(T_e^* - T_e) > \Delta T_e$	1 ↑
$-\Delta T_e < (T_e^* - T_e) < \Delta T_e$	0
$(T_e^* - T_e) < -\Delta T_e$	-1 ↓

Table 3: Voltage vector selection

Hysteresis comparator output	Sector selection					
	1	2	3	4	5	6
$\Delta\Psi$	ΔT_e					
1 ↑	1 ↑	V ₂	V ₃	V ₄	V ₅	V ₆
	0	V ₇	V ₀	V ₇	V ₀	V ₇
	-1 ↓	V ₆	V ₁	V ₂	V ₃	V ₄
	1 ↑	V ₃	V ₄	V ₅	V ₆	V ₁
-1 ↓	0	V ₀	V ₇	V ₀	V ₇	V ₀
	-1 ↓	V ₅	V ₆	V ₁	V ₂	V ₃

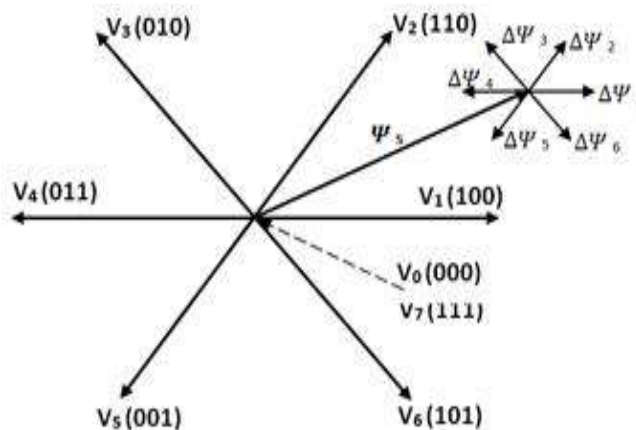


Fig. 2: Voltage sectors and stator flux vectors

Voltage vector selection: The voltage vectors are selected based on the hysteresis comparators output and stator flux position $\theta_e(k)$. Figure 2 shows the stator flux and voltage vectors. There are six active voltage vectors (V_1 to V_6) and two zero vectors (V_0, V_7). If stator flux is in sector1, for a small increase in flux and large increase in torque vector V_2 has to be selected using the Table 3. The vector selection is similar for stator flux is in other sectors.

RESULTS AND DISCUSSION

The proposed system is modelled and simulated using MATLAB/SIMULINK platform. The simulation results have been presented for varying load and wind speed conditions and under stator terminals short circuited condition. The inductance machine is rated for 2.2 kW, 415 V, 50 Hz. The voltage build-up of the SEIG under no load condition for a wind speed of 9 m/sec is shown in Fig. 3. The required reactive power for the initial excitation of SEIG is supplied using battery through the VSC.

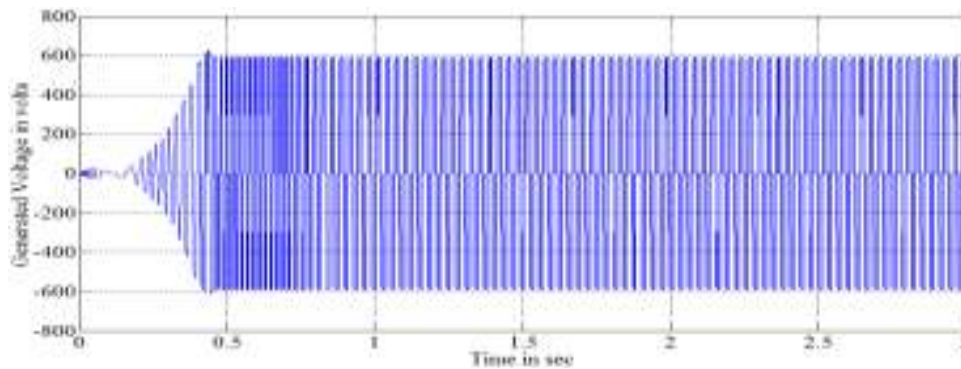
The terminal voltage of the SEIG reaches the battery voltage, diode D gets reverse biased and blocks the power flow from the battery to the generator. At time $t = 0.4$ sec, the terminal voltage reaches 596 V and due to the magnetic core saturation of SEIG, the voltage gets maintained at the reference value.

During the voltage build-up of the SEIG generator, at $t = 0.3$ sec the wind speed is reduced from 9 m/sec to

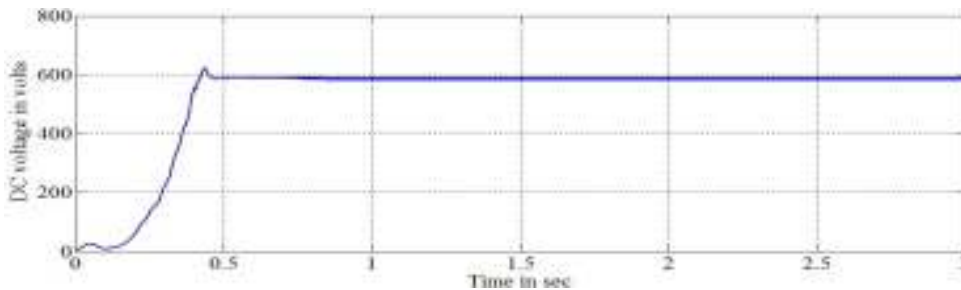
5 m/sec which results decrease in rotor speed of the generator. Therefore, there is a drop in generator terminal voltage which in turn decreases the magnetizing inductance. The decrease in magnetizing inductance further reduces the voltage. Finally, the voltage drops to zero is shown in Fig. 4. The change in voltage is not instantaneous because of the inertia of the rotating parts. At $t = 1$ sec, the wind speed is increased to 9m/sec, the voltage stays remain at zero. Once, the voltage drops to zero, there is no transient response. The demagnetization of core will occur, therefore, there would not be any self-excitation until the core has to be re-excited.

Response with load: During the voltage build-up of SEIG, the load of 3kW is applied at $t = 3$ sec, the stator current increases to high value and then falls to zero which results in complete collapse of the voltage build up. Finally the generator voltage reaches to zero. The generator voltage and stator current waveforms are presented in Fig. 5.

Response of SEIG during Short circuited terminals: The induction generator is driven at constant speed, the stator terminals are short circuited at $t = 2$ sec, then there is a collapse in the generator terminal voltage. Suddenly, the stator current rises to a high value and then drops to zero are shown in Fig. 6. This shows the induction generator has inherent capability of self-protection against short circuit.



(a)



(b)

Fig. 3: Voltage build-up of SEIG under no load; (a) Terminal voltage of SEIG, (b) DC voltage

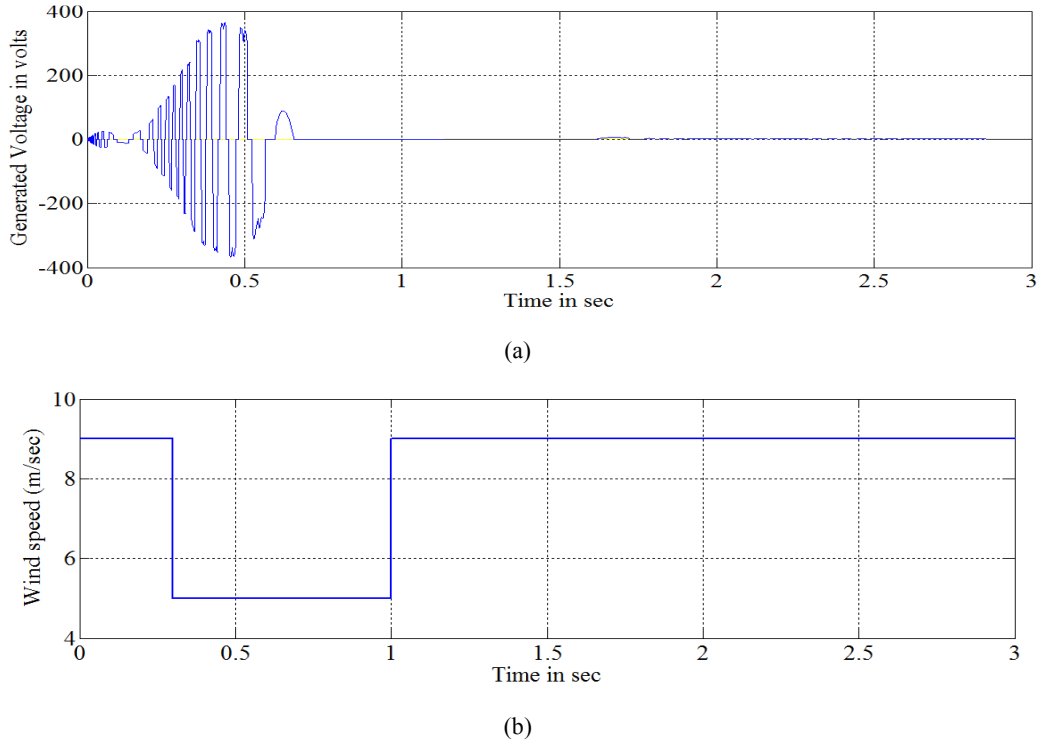


Fig. 4: SEIG terminal voltage during drop in speed; (a) Generator voltage, (b) wind speed

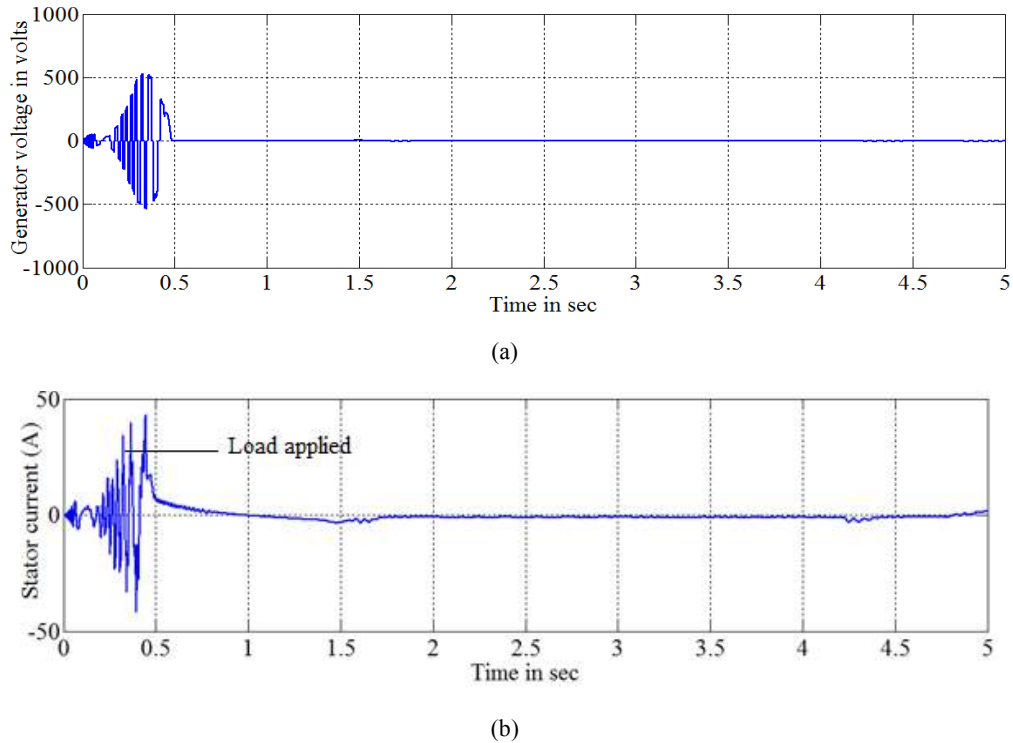
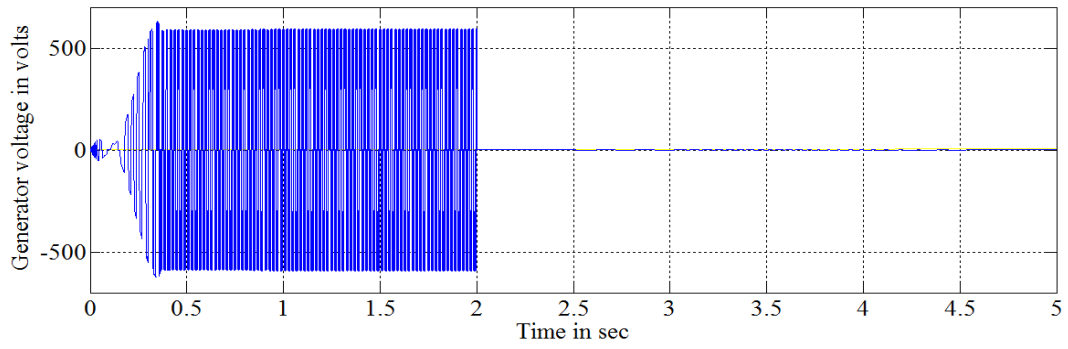
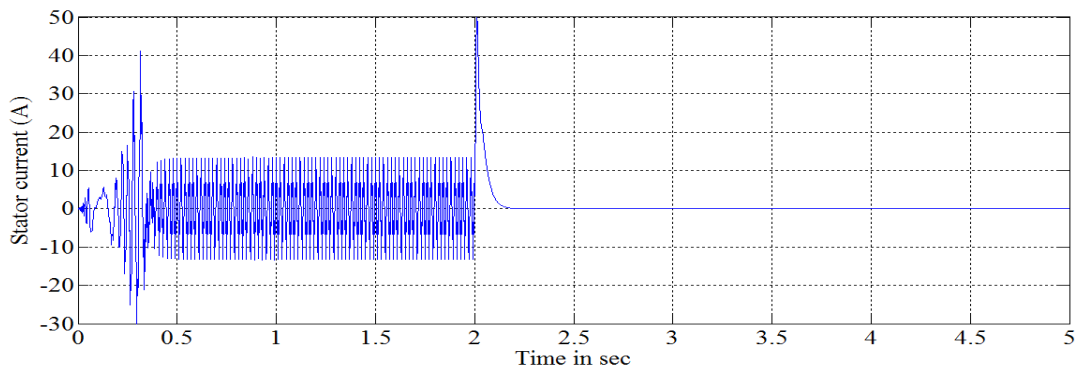


Fig. 5: Generator terminal voltage and stator current during voltage build-up under loaded condition; (a) Generator voltage, (b) stator current

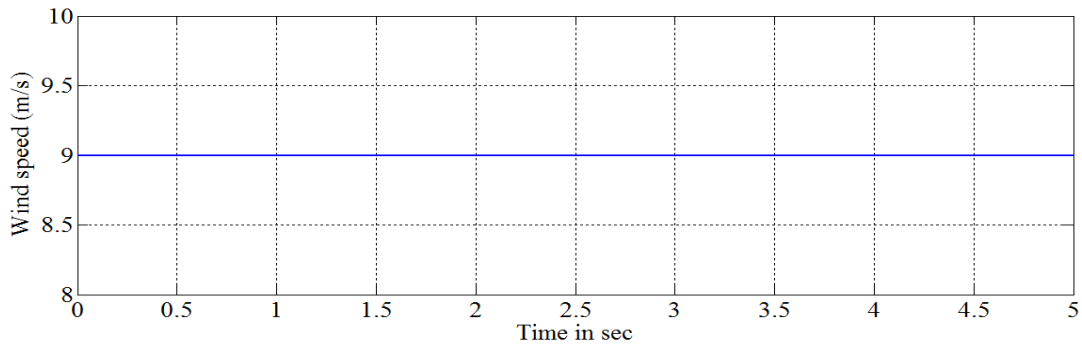
Response of SEIG with step change in load: At $t = 0$ sec, the VSC with battery are connected across the stator terminals of the SEIG. The SEIG starts build-up the voltage and it reaches to the steady state value at $t = 0.4$ sec. Initially, the frequency is 51Hz which is measured using phased locked loop.



(a)

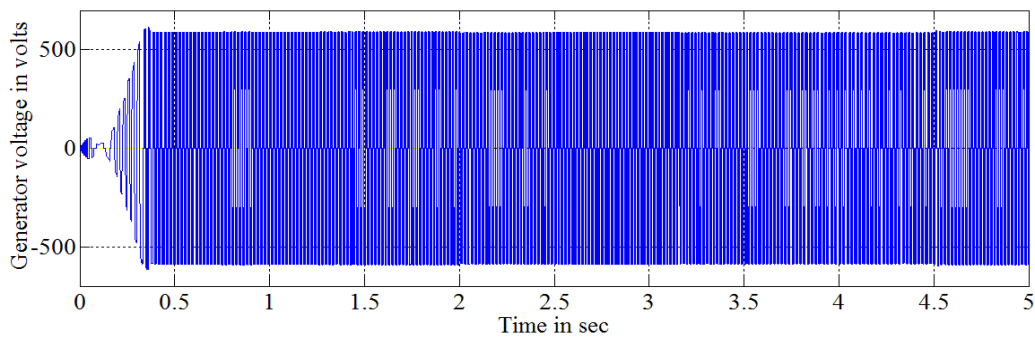


(b)

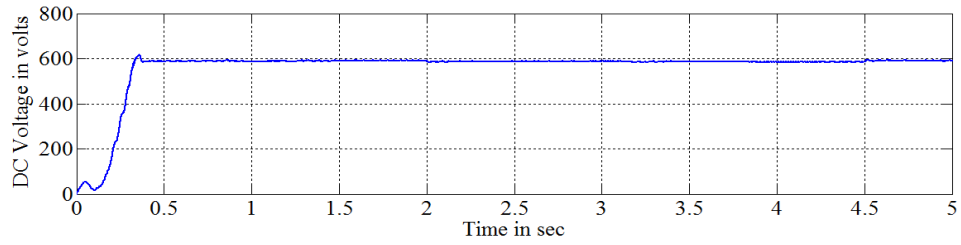


(c)

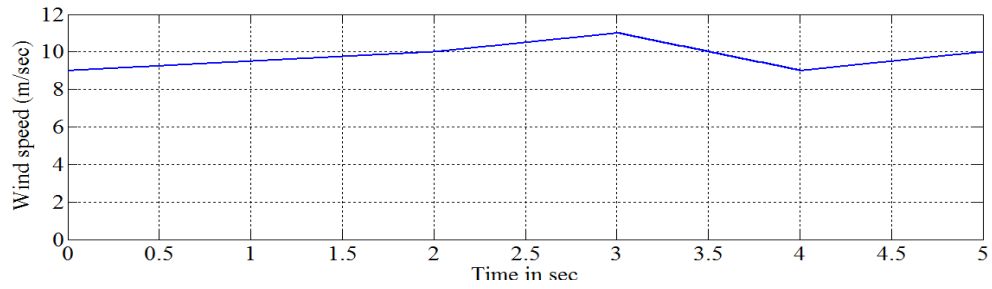
Fig. 6: Response of SEIG when the stator terminals short circuited; (a) Generator voltage, (b) stator current, (c) wind speed



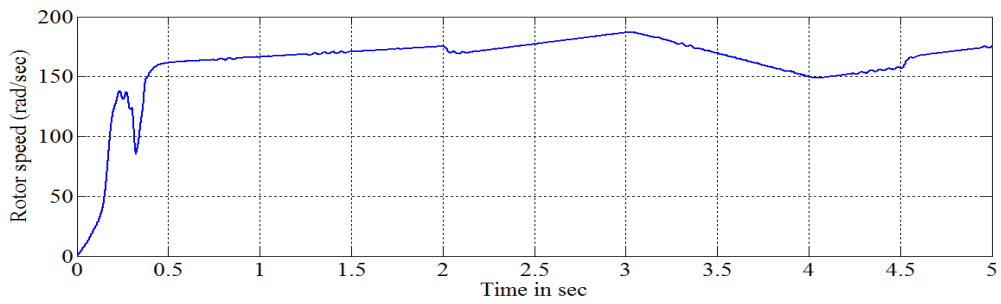
(a)



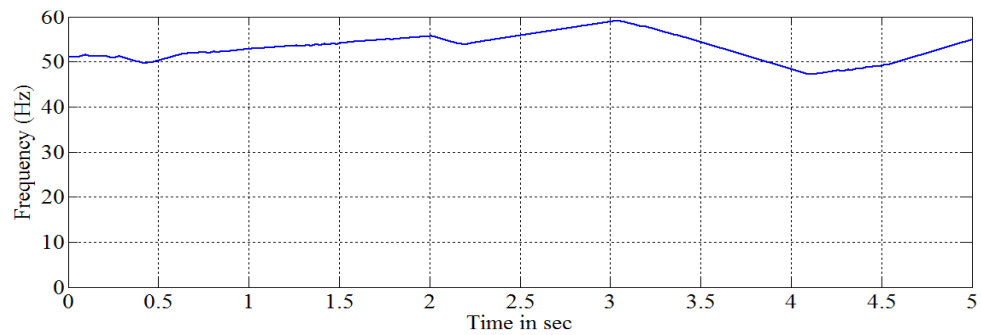
(b)



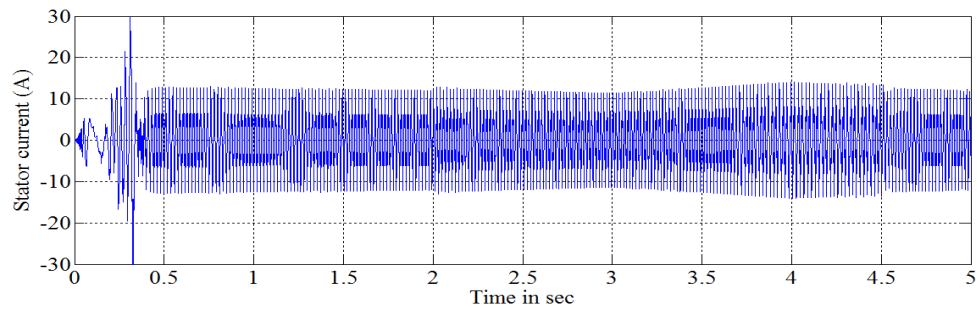
(c)



(d)



(e)



(f)

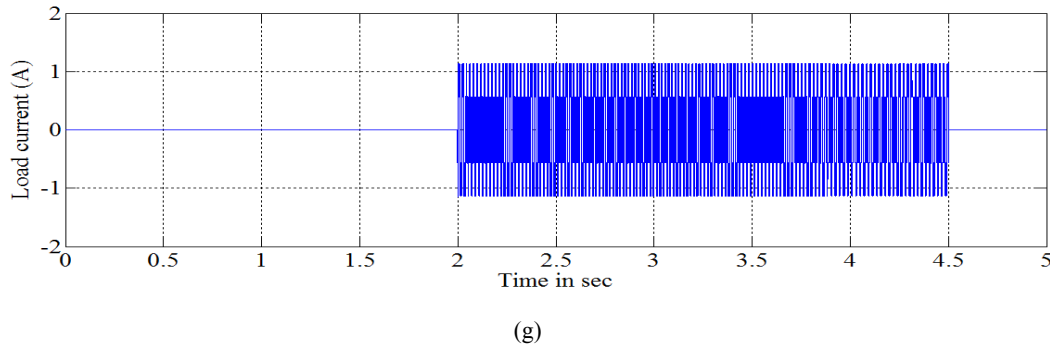


Fig. 7: SEIG characteristics under variable speed and step change in load conditions; (a) generator voltage, (b) DC voltage, (c) wind speed, (d) rotor speed, (e) frequency, (f) stator current, (g) load current

At this condition, no load is connected across the SEIG terminal. The various parameters of SEIG are presented in Fig. 7.

At time $t = 2$ sec, the unity power factor load of 700W is applied and also the speed is changed from 9m/sec to 10m/sec linearly. The generator terminal voltage and DC voltage is maintained constant. The load current and stator current are increased. The generator rotor speed changes uniformly with wind speed. The stator frequency increases due to the availability of excess power in the rotating parts.

At $t = 3$ sec, the wind speed is decreased from 11 m/sec to 9 m/sec linearly. The generator terminal voltage and DC voltage is maintained constant. The stator current is increased to meet the power demanded by the load. The generator rotor speed decreases uniformly with wind speed. The stator frequency also decreases.

At $t = 4$ sec, the wind speed is raised from 9 m/sec to 10 m/sec linearly. The stator current decreases whereas the rotor speed and stator frequency increases.

At time $t = 4.5$ sec, the load is disconnected from the generator. There is a slight increase in voltage due to the availability of excess power and then it settles to the reference value. The stator current reaches to the no load value. The rotor speed and stator frequency increases. Therefore, SEIG is suitable where the electrical equipment is insensitive to frequency variation such as heater, battery charger, lighting, water pumping and power remote islands etc.

CONCLUSION

The dynamic performance of self-excited induction generator driven by a variable speed wind turbine has been analysed for varying load and wind speed conditions and short circuit at stator terminals using direct torque control strategy. The advantages of using direct torque control strategy for wind energy conversion system is that, only the stator resistance is needed for the estimation of stator flux and torque. The simulation results show that the generator terminal voltage is maintained constant for variable wind speed and loading conditions.

REFERENCES

- Aymen, F. and S. Lassaad, 2012. A new adaptive high speed control algorithm used for a FOC or a DTC PMSM drive strategies. Proceeding of 38th Annual Conference on IEEE Industrial Electronics Society. Montreal, QC, October 25-28, pp: 4472-4476.
- Bose, B.K., 2003. Power Electronics and AC Drives. Englewood Cliffs, Prentice-Hall, NJ.
- Daniel, S.A. and N. Ammasaigounden, 2004. A novel hybrid isolated generating system based on PV fed inverter-assisted wind-driven induction generators. IEEE T. Energy Convers., 19(2): 416-422.
- Depenbrock, M., 1988. Direct self-control (DSC) of inverter-fed induction machine. IEEE T. Power Electr., 3(4): 420-429.
- Grantham, C., D. Sutanto and B. Mismail, 1989. Steady-state and transient analysis of self-excited induction generators. IEE Proc-B, 136(2): 61-68.
- Honorati, O., G.L. Bianco, F. Mezzetti and L. Solero, 1996. Power electronic interface for combined wind/PV isolated generating system. Proceeding of the European Union Wind Energy Conference. Goteborg, Sweden, pp: 321-324.
- Infield, D.G., G.W. Slack, N.H. Lipman and P.J. Musgrove, 1983. Review of wind/diesel strategies. Proc. Inst. Elec. Eng. A, 130(9): 613-619.
- Jayaramaiah, G.V. and B.G. Fernandes, 2006. Novel voltage controller for standalone induction generator using PWM-VSI. Proceeding of IEEE Industry Applications Conference. USA, 1: 204-208.
- Korkmaz, F., I. Topaloglu, M.F. Cakir and R. Gurbuz, 2013. Comparative performance evaluation of FOC and DTC controlled PMSM drives. Proceeding of IEEE 4th International Conference on Power Engineering, Energy and Electrical Drives. Istanbul, May 13-15, pp: 705-708.
- Krause, P.C., O. Wasynczuk and S.D. Sudhoff, 2002. Analysis of Electric Machinery and Drive Systems. 2nd Edn., John Wiley and Sons, New York.

- Lee, B.K. and M. Ehsani, 2001. A Simplified functional simulation model for a three phase voltage source inverter using switching function concept. *IEEE T. Ind. Electron.*, 48(2): 309-321.
- Leidhold, R., G. Garcia and M.I. Valla, 2002. Field-oriented controlled induction generator with loss minimization. *IEEE T. Ind. Electron.*, 49: 147-155.
- Mateo, B. and D. Vukadinovic, 2013. Vector control system of a self-excited induction generator including iron losses and magnetic saturation. *Control Eng. Pract.*, 21: 395-406.
- Ojo, O. and I.E. Davidson, 2000. PWM-VSI inverter assisted stand-alone dual stator winding induction generator. *IEEE T. Ind. Appl.*, 36: 1604-1611.
- Patil, U.V., H.M. Suryawanshi and M.M. Renge, 2014. Closed-loop hybrid direct torque control for medium voltage induction motor drive for performance improvement. *IET Power Electron.*, 7: 31-40.
- Seyoum, D., M.F. Rahman and C. Grantham, 2003. Terminal voltage control of a wind turbine driven isolated induction generator using stator oriented field control. *Proceeding of 18th Annual IEEE Applied Power Electronics Conference and Exposition. USA*, 2: 846-852.
- Takahashi, I. and T. Noguchi, 1986. A new quick-response and high efficiency control strategy of an induction motor. *IEEE T. Ind. Appl.*, 22: 820-827.
- Vas, P., 1998. *Sensorless vector and Direct Torque Control*. Oxford University Press, Oxford.